THE USE OF ACTIVE CONTOURS FOR THE DETECTION OF COASTLINES IN SAR IMAGES: A MODULAR KNOWLEDGE-BASED FRAMEWORK

Benjamin Seppke, Leonie Dreschler-Fischer, and Max Brauer

University of Hamburg
Department of Informatics
Cognitive Systems Laboratory
{seppke, dreschler, 5brauer}@informatik.uni-hamburg.de

KEY WORDS: SAR, coastal, coastlines, segmentation, computer vision, intertidal flats, Wadden Sea

ABSTRACT:

Over the last years, active contour methods have become a basic tool in computer vision. They have proven to be efficient for various image processing applications, like reconstruction of the edges inside images or the tracing of image features. However, when applying the basic snake technique to synthetic aperture radar (SAR) remote sensing images, the detection of edges may not be satisfactory. This is caused by the special imaging technique of SAR that may tend to produce varying-contrast edges and the commonly known speckle noise. In (Seppke et al., 2010) we proposed the use of asymmetric external energy terms to cope with these problems. In this paper we extend our approach and present a modular framework for the application of snake algorithms to SAR imagery. The main emphasis of the framework is the use of higher knowledge about the scene depicted, e.g to initialize the snake with suitable parameters. Another objective is to establish a modular designed and thus highly flexible testbed for the comparison of different active contour approaches. We present the framework's design and preliminary results for the detection of coastlines in SAR images. The proposed framework has already proven to be a valuable tool for both, the interpretation and understanding of the results. For future projects, the framework will be used to investigate and compare the results of snakes when applied to hi-resolution SAR imagery, e.g. TerraSAR-X HR Spotlight images.

1 INTRODUCTION

The detection and accurate localization of edges in remote sensing data is one of the most important tasks in image processing. These edges are usually boundaries between imaged objects, and thus can be used for the segmentation of these objects. In contrast to region based approaches, many boundary based segmentation approaches evolved in the past decades. (Gonzalez and Woods, 2006) gives a good overview of the different approaches. One main challenge of edge localization is the extraction of long connected boundaries from real-world image data. Due to the basic definition of an images' gradient, it may be locally impossible to determine if a boundary is existent or not.

To extract connected boundaries, active contour algorithms have been introduced by (Kass et al., 1987). They describe boundaries by means of linear (open or closed) structures. Contrary to commonly known local pixel based approaches, they take advantage of both the connectivity of the structure and the image gradient information in conjunction. They have proven to be efficient for the localization and tracking of linear structures at a sub-pixel accuracy. According to their definition, active contour approaches are capable to bridge those gaps in the image gradient information. This is achieved by an energy term, which favors smooth, connected curves and thus penalizes too much bending. The energies are usually defined such that the contour will iteratively fit to image edges or other features of interest inside the image during the optimization process. This behavior seems to be the reason for their commonly used synonym: *snakes*.

From former studies, we noticed that the definition of the snake and the optimization strategy may vary if the task, the data, or both are changing. The accurate localization of varying contrast edges in synthetic aperture radar (SAR) images may e.g. require the introduction of a new asymmetric external energy term (Seppke et al., 2010).

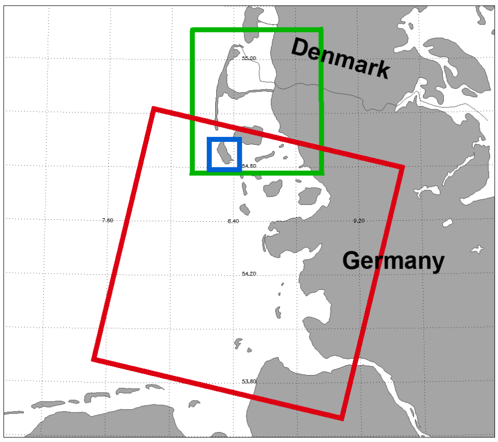

Figure 1: The area of interest: The German Bight (North Sea) showing the northern part of the Wadden Sea. red: image acquisition area of the used data, green, boundary of the ENC, blue: ROI used for this work (around the island of Amrum).

In this work, we present a highly-flexible and interactive framework, which encapsulates the different possibilities by means of modules that can be selected and replaced interactively. In addition to the flexibility of the algorithms, we add a mechanism to initialize the snake with higher scene knowledge. These higher knowledge can e.g. be used to initialize the snake and to inspect the results. As an example, we have selected the accurate localization of coastlines based on SAR imagery. The image has been acquired by the ERS 2-SAR on 24th July, 2008 at 10:25 UTC and shows the German UNESCO Heritage Site "Wadden Sea". In this image, the coastlines show up as boundaries between a homogeneously imaged water surface on one hand and a heterogeneous silt surface on the other hand. This makes it nearly impossible to estimate the land-water boundaries using common edge detectors like the canny edge detector, texture based methods (Onana et al., 2001), or classical SAR shoreline detection algorithms (Tan et al., 2005). As a first knowledge source, we present a connection between an electronic nautical chart (ENC) and the framework by means of snake initialization.

This paper is organized as follows: First we briefly introduce the formal background of active contours. We will then describe the requirements and design issues that yield to the proposed framework and will give an impression of first coastline detection results. We conclude with a discussion of the results and end up with an outlook concerning future work and other applications.

2 ACTIVE CONTOURS

We refer to a snake as a parametric curve that is geometrically embedded into a two-dimensional plane $\vec{s}(p) = [x(p), y(p)]$ with $p \in [0, 1]$. To model the parametric curve, we used a B-Spline approximation of n given control points. This approximation has some advantages over other approximations (Brigger et al., 2000). As the active contour needs to fit to some linear features of the image, we define an energy functional which shall be minimized during the snakes' optimization:

$$E(s) = \int_0^1 E_{int}(p) + E_{ext}(p)\, dp \tag{1}$$

where E_{int} is the internal energy of the snake, which describes the internal shape constraints, and E_{ext} denotes the external energy that is caused solely by the image (e.g. by means of the image gradient). The iterative minimization of the functional given in eq. (1) causes the snake to move with respect to the given energy constraints.

In this work, we are focussing on the application of snakes in a knowledge-based and modular framework, and will not go into detail of the snakes' theoretical background. More information on this can be found in (Kass et al., 1987). We will now discuss a few possible energy terms, which can be used for both the internal and the external energy, in more detail.

2.1 Energy Definitions

Both energy parts E_{int} and E_{ext} can be defined in various ways, depending on the task and on the image data. We start with a brief introduction to commonly used definitions of the internal energy E_{int}, which represents the intrinsic energy of the snake and is often differentiated into two internal energy parts:

$$E_{int} = a_s E_s + a_c E_c \tag{2}$$

The strength of the different energy terms is controlled by the two coefficients a_s, the spacing coefficient, and a_c, the linearity coefficient, which controls the strength of the curvature dependent term. The internal spacing energy E_s is given by:

$$E_s = \sum_{i=0}^{n-2} \left(\frac{|\vec{d_i}|}{l} - 1 \right)^2 \tag{3}$$

where the vectors $\vec{d_i}$ denote the differences between two neighbored control points $\vec{c}_{i+1}$ and $\vec{c}_i$. There are n control points, which yield $n-1$ difference vectors; l gives the goal length for the segments. This segment length is a parameter of the snake as well and may be set programmatically (e.g. to the average segment length). E_s will be zero if and only if all the segments have a length of l. It will approach $n-1$ if the snake shrinks to a point and will grow with the square of the length of the snake as it is stretched further and further. The curvature dependent term E_c is given by:

$$E_c = \sum_{i=0}^{n-3} \left(1 - \frac{\vec{d_i} \cdot \vec{d}_{i+1}}{|\vec{d_i}||\vec{d}_{i+1}|} \right) \tag{4}$$

This energy will be in the range $[0, 2(n-2)]$. A value of zero signals a straight line and the more the snake is bent the higher this energy becomes.

One basic definition of the external energy E_{ext} is given by the image gradient under the snakes geometrical embedding. For the simple case, we can define the energy as the inverse gradient magnitude:

$$E_{ext} = \sum_{i=0}^{n-1} \frac{1}{\nabla I_s(\vec{s}(p_i))^2} \tag{5}$$

where $\nabla I_s(\vec{s}(p_i))^2$ denotes the image gradient magnitude at position $\vec{s}(p_i)$. This edge detector is applied to the image at all points of the snake and rotated to match the snake's direction. All filter responses are squared and summed up to obtain the edge related energy term E_{ext}. This allows the snake to find dark/bright as well as bright/dark edges. However, when just one type of edges (e.g. dark to bright) is allowed, we can model this by scalar multiplying the snakes normal vector $\vec{n}_i$ at a given snake position p_i with the gradient direction at this position:

$$E_{ext} = \sum_{i=0}^{n-1} \nabla I_s(\vec{s}(p_i)) \cdot \vec{n}_i \tag{6}$$

Recent studies have shown that it may be necessary to add further energy terms when applying the snakes on SAR imagery (Seppke et al., 2010). This is caused by the strong speckle noise of the images and some domain specific features of the tasks, e.g. that water sometimes appears quite smooth in a SAR image since the wind and hence the waves do not change on a small scale. When adding other energy terms, the user needs to determine the ratio of each energy compared to the other. For the simple case of two different external energy parts, which are normalized, one parameter α may be used as the relative weight:

$$E_{ext} = \alpha E_{ext1} + (1 - \alpha) E_{ext2} \tag{7}$$

If alpha is set to zero, only the edge detecting energy will be used. Contrary, a value of one leads to a use of only the variance dependent term.

2.2 Optimization Strategy

To minimize the overall energy E of eq. (1), several optimization approaches can be used. So far, iterative algorithms have yielded good results. Although there are several different iterative approaches possible, we will focus on gradient back step algorithms based on a variation of the control points. We distinguish between two different superior optimization concepts, which are mainly independent of the actual iterative approach: single- and multi-grid approaches.

A single grid optimizer uses the full image resolution during the complete optimization. This may be problematic, e.g. if the distance between the initial snake and the estimated final position is quite large. To solve the problem of large distances, multi-grid approaches have been developed. These approaches refer to the image at different scales, and optimize the snake on these scales. Thus, for these approaches a scale space of the image needs to be build a priori.

3 TOWARDS A MODULAR FRAMEWORK

The existence of different energy terms and optimization strategies implies a modular framework design. Instead of an inflexible task-tailored solution, which works well for exactly one task, our aim is to provide support for an easy adaptation to different tasks. From section 2.1 follows that it may be necessary to calculate not just the magnitude but also the direction of the image's gradient. In addition to the gradient vector, normals along the snake may have to be defined. If we want to support all possible configurations we need to encapsulate the different possible algorithms in different modules.

Besides the different snake definitions, the user should be supported by means of scene knowledge. For the task of detecting coastlines, we propose the use of S-57 electronic nautical charts (ENCs) for snake initialization. The ENCs used herein have been provided by the German Federal Maritime and Hydrographic Agency. More information about the structure and contents of these ENCs can be found in (IHB, 1996). This is just one of many possible knowledge sources – the framework should not be restricted to this one.

3.1 Requirements for the framework

We now present the main ideas behind the development of the framework by means of the requirements and their implications into the development process. The main requirement is the modularity in conjunction with a fast first framework development result. Thus, we need to consider agile and highly flexible object oriented rapid prototyping design patterns (Dingsyr et al., 2010).

The basis of the framework should be flexible using prototype classes for common tasks. The first prototype may integrate only one knowledge source, but needs to be designed open to include others in future. We do not reinvent the wheel but need to find and integrate external libraries and extensions for commonly known basic tasks into our framework. There are two main needs for external libraries: fast image processing algorithms, which we need to apply even for large images and the import of higher scene knowledge. The framework itself is considered to be freely available and platform-independent.

To conclude the framework's requirements, we want to emphasize the two main aspects: it should be easy to learn for end-users and be easy to extend by developers. The first point yields to a comprehensive graphical user interface, which should be self-explaining and clearly designed. The second aspect yields to well-designed modular and thus flexible source code of the framework.

3.2 A first framework

Because of the good rapid prototyping performance, we have decided to use the interactive Python programming language to implement our framework. For different scientific calculations, the scientific extension SciPy is used in conjunction with the numeric array extension NumPy. This constellation has already proven to be adequate for the processing of scientific tasks (Luszczek and Dongarra, 2006). Due to the interactivity of the programming language, new approaches or minor modifications of existing approaches can be tested interactively without restarting or recompiling the program. We use the object-oriented approach of classes in Python to abstract from concrete algorithms by providing prototypes for each snake setting. This makes the framework highly extensible while maintaining the clarity and readability of the source code.

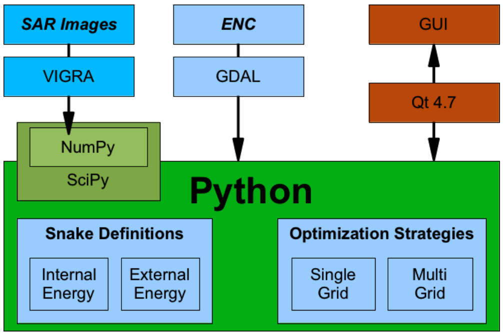

Figure 2: The components of the first framework. Python in conjunction with NumPy and SciPy forms the basis, Qt is used for interaction, VIGRA and GDAL for external image and ENC access. Data sources are highlighted italic bold and interchangeable modules are filled with light blue color.

To meet the requirement of fast and reliable image processing algorithms, like the building of a scale-space or the fast and accurate calculation of image gradients, we use the current VIGRA 1.7.1 library. VIGRA stands for *Vision with GeneRic Algorithms* and is a template based C++ library, which comes with Python-NumPy bindings. The images are internally represented by means of NumPy arrays. As a first knowledge source, we use S-57 ENCs, which we read into the system using the geographical data abstraction library (GDAL). The GDAL library also provides a Python wrapper for interactive usage.

To give the user the opportunities of controlling the framework graphically and performing visual inspection of the results, we developed an interactive graphical uses interface (GUI) using the Qt 4.7 framework and the corresponding Python bindings. This allows for a platform independent implementation, at least on the three most popular operating systems: Windows, Linux, Mac. Figure 2 shows the different components of our framework. Note that the light blue filled rectangles correspond to prototypes and thus can easily be extended or be replaced. During the GUI design phase, we kept attention on two aspects: simplicity and clarity. As it is shown in fig. 3, the controls on the left side are ordered by their meaning and role in the process of coastline detection. This provides a powerful but easy to use interface.

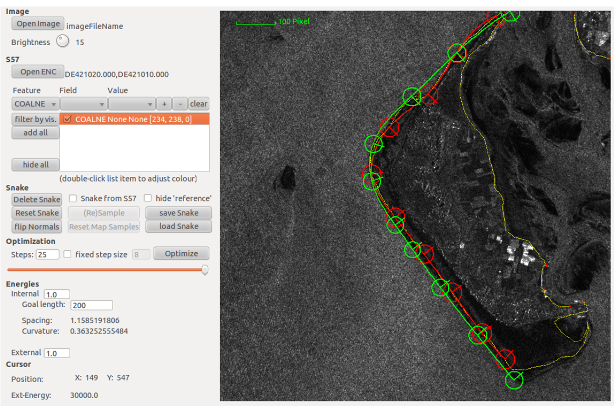

Figure 3: Overview of the current framework with controls on the left and an interactive view (showing the island of Amrum) on the right. After the optimization of the initial snake (red), all optimization steps can be visualized using a slider widget.

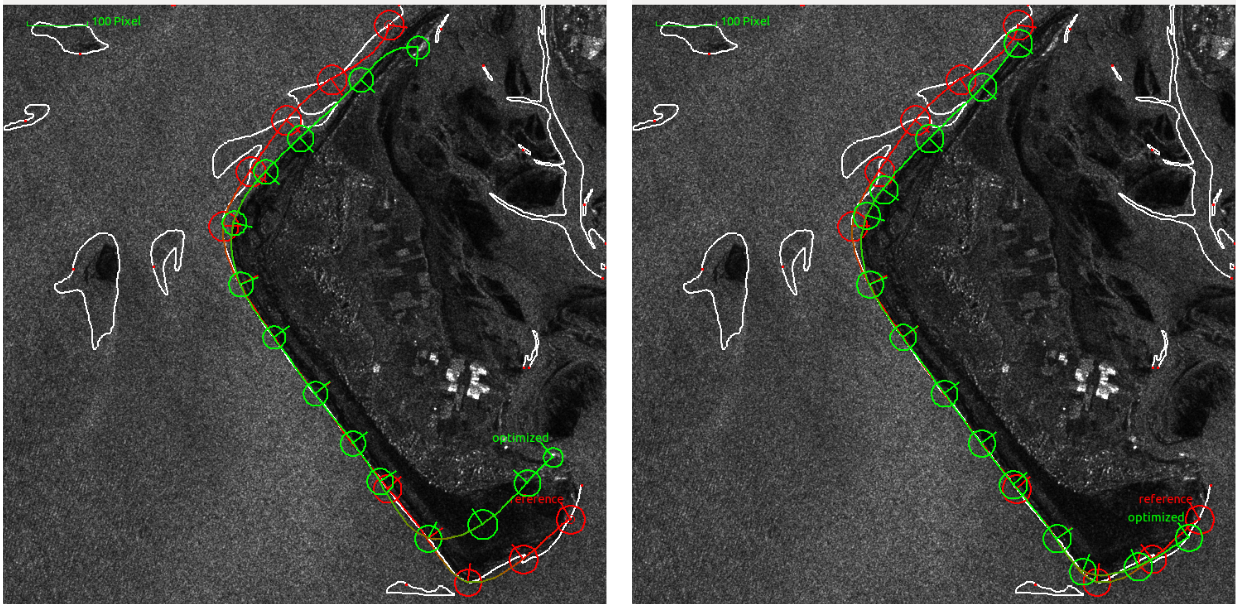

(a) Gradient magnitude based external energy of eq. (5) (b) Gradient direction based external energy of eq. (6)

Figure 4: Two resulting views of the proposed framework using different external energy terms and and an initialization using S-57 ENCs. The zero-level waterlines are printed in white. The initial snake is printed in red, whereas the finally optimized snake is printed in green. The positions of the control points are marked by circles, whereas lines visualize the user-defined normal directions at the control points. The changing color along one contour is caused by the varying inner tension due to the inner energy definition of the snake. Further information about the parameters are given in section 4.

4 RESULTS AND DISCUSSION

We will now present first results, which have been produced using the framework. The task is to accurately locate water/land boundaries in intertidal flat areas like the "Wadden Sea" (see section 1). We have selected the western coastal boundary of the island of Amrum as a first example for this work, as it is depicted in fig. 1. Because of the continuous flooding and dry-falling of land during each tidal cycle, the coastline may largely vary due to the time of the image acquisition. The image we used, was taken about 15 minutes before low tide. showing some dry-fallen areas at the eastern part of fig. 4, which have resulted in a minor radar reflection than the surrounding sea surface.

For the initialization of the snake, we have used data of the S-57 ENC, namely the zero-level waterline, which is encoded by the *DEPCNT* feature with a value *VALDCO=0.0*. The corresponding feature lines are marked white in fig. 4. Another important ENC feature is named *COALNE* and refers to coast lines. These lines are highlighted yellow in fig. 3 but have been left out in fig. 4 for a better visualization. Note that the current "coastline" by means of a boundary between water and land is different to the coastline of the ENC due to the low-tide conditions at which the scene was acquired.

Our aim is to analyze the influence of the different external energy terms of eq. (5) and eq. (6) respectively. Therefore, we used the same weighting values for the internal energy for both cases, according to eq. (2):

$$E_{int} = 0.175E_s + 0.175E_c$$

which results in lower weighting of the internal energy term. This allows for a more flexible snake behavior. Additionally, we define a target distance between the control points of the snake of 100 pixels. We use only one external energy per case, hence there is no need for an external weighting factor α.

The optimization approach is the same for both test cases. We have chosen a multi-grid gradient back step optimization approach, which is working on 5 scales of the image. Each scale is derived by a convolution of the image with a gaussian filter of corresponding standard deviation σ. This has been performed iteratively to save creation time. The scales are:

$$S_\sigma = \{6, 12, 18, 24, 30\}$$

The optimization is carried out by 25 iterations overall, which results in 5 optimization steps per scale. Inside one scale $s \in S_\sigma$ we use a step size of s for the optimization and thus motion of the snake.

The left panel of fig. 4 shows the result when using the gradient magnitude based external energy term of eq. (5). We notice a good detection of the longer western waterline on one hand, but also see some erroneous localization on the northern and southern tip of the island. These differences are caused by strong gradient magnitudes at that areas. The gradient magnitudes are higher than those of the land-water-boundary and thus attract the snake.

On the right panel of fig. 4 we see the result obtained when using the gradient normal vector based external energy term of eq. (6). The use of the gradient's normal vector lead to a very accurate localization of the boundary. Contrary to the results of the gradient magnitude based external energy, the snake has not been attracted by gradients of high magnitude because of the different direction of the gradient. We also recognize that the initialization of the snakes using knowledge from ENCs is a very valuable feature because it allows for automated approaches and does not lead to error caused by the fine sampling of control points.

5 CONCLUSIONS AND FUTURE WORK

We presented the design of a modular and flexible framework, from the task up to first results. The framework meets all requirements posed to it so far. Furthermore, it is not restricted to one special task in a special domain, but allows for easy adaptation to other domains. According to all the requirements described in section 3.1, we only presented one possible implementation. It might of course be possible to use other tools or programming languages to fulfill the requirements.

The user can then try different approaches and compare the results visually. As all optimization states of the snake are stored, it is easy to inspect the behavior of the snake or at least to figure out when the snake did deviate too much from the desired result. For further investigation, the user may look at the energies of the snake at that optimization step and select other energy terms for the next run.

The first results of the framework look very promising, and the modular design of the framework supported the very short design and implementation cycle. The framework assists in easy comparison and thus leads to a better understanding of the resulting coastlines. For the future, we plan to implement and test other energy terms and optimization strategies. We will also perform tests with newly acquired high resolution SAR data of coastal areas in near future.

ACKNOWLEDGEMENTS

The authors are grateful to Martin Gade for his support in interpretation of coastal SAR images of the “Wadden Sea” and to the German Federal Maritime and Hydrographic Agency (BSH) for the providing of ENCs for research purpose. This work is partly supported by the German national project DeMarine (50 EE 0817).

REFERENCES

Brigger, P., Hoeg, J. and Unser, M., 2000. B-Spline Snakes: A Flexible Tool for Parametric Contour Detection. IEEE Trans. on Image Processing 9(9), pp. 1484–1496.

Dingsyr, T., Dyb, T. and Moe, N. B., 2010. Agile Software Development: Current Research and Future Directions. 1st edn, Springer Publishing Company, Incorporated.

Gonzalez, R. C. and Woods, R. E., 2006. Digital Image Processing (3rd Edition). Prentice-Hall, Inc., Upper Saddle River, NJ, USA.

IHB, 1996. Iho transfer standard for digital hydrographic data, edition 3.0. Technical Report Special Publication 57, International Hydrographic Bureau.

Kass, M., Witkin, A. and Terzopoulos, D., 1987. Snakes: Active Contour Models. In: Proc. of 1^{st} ICCV, London, England, pp. 259–268.

Luszczek, P. and Dongarra, J., 2006. High performance development for high end computing with python language wrapper (plw. International Journal of High Perfomance Computing Applications.

Onana, V., Mvogo Ngono, J., Trebossen, H., Rudant, J. and Tonye, E., 2001. Coastline detection in SAR images using texture analysis in textural or geometrical multi-resolution. In: Geoscience and Remote Sensing Symposium, 2001. IGARSS ’01. IEEE 2001 International, Vol. 3, pp. 1549–1551 vol.3.

Seppke, B., Dreschler-Fischer, L. and Hübbe, N., 2010. Using snakes with asymmetric energy terms for the detection of varying-contrast edges in sar images. Pattern Recognition, International Conference on 0, pp. 2792–2795.

Tan, Q., Liu, Z., Fu, Z. and Hu, J., 2005. Lake shoreline detection and tracing in SAR images using wavelet transform and ACM method. In: Geoscience and Remote Sensing Symposium, 2005. IGARSS ’05. Proceedings. 2005 IEEE International, Vol. 5, pp. 3703–3706.